JOURNAL OF SOLID STATE CHEMISTRY 66, 256–262 (1987)

Phase Diagram and IR Spectral Investigations of the $2TeO_2 \cdot V_2O_5$–$Li_2O \cdot V_2O_5 \cdot 2TeO_2$ System

VESSELIN DIMITROV

Higher Institute of Chemical Technology, Sofia 1156, Bulgaria

Received January 6, 1986; in revised form June 6, 1986

By means of X-ray phase analysis, IR spectroscopy, and DTA, the system $2TeO_2 \cdot V_2O_5$–$Li_2O \cdot V_2O_5 \cdot 2TeO_2$ was investigated and its phase diagram was constructed. The formation of a new compound with composition $Li_2O \cdot 3V_2O_5 \cdot 6TeO_2$, melting incongruently was documented. A comparison of the bands in the IR spectrum was made. Stable glasses in the whole range of concentrations were prepared. From the IR spectra of the glasses, the corresponding crystallization products, and the data of known crystal structures, a model of the short-range order in the glasses was proposed.

Introduction

Compounds of the $Me_2O \cdot V_2O_5 \cdot 2TeO_2$ (MVT_2) type in the M_2O–V_2O_5–TeO_2 system were reported by Darriet *et al.* (*1*). In our earlier work on this system we reported (*2–4*) another ternary compound of the type $Me_2O \cdot 3V_2O_5 \cdot 6TeO_2$ (MV_3T_6), where Me = Na, K, Ag. The aim of the present work was to investigate the $2TeO_2 \cdot V_2O_5$–$Li_2O \cdot V_2O_5 \cdot 2TeO_2$ (T_2V–LVT_2) system, about which no data are available in the literature.

Experimental

The phases T_2V and LVT_2 were synthesized by the method described in (*2*) with TeO_2 (Merck), V_2O_5 (Renal), and Li_2CO_3 (p.a.). The compounds so obtained were used for the preparation of batches in the range from 0 to 100 mole% for every 5 mole% LVT_2. The homogenization of each composition was carried out for 20 min in an agate mortar while the material was molten at 700–750°C. Some of the glasses were subjected to mass crystallization at T = 300–350°C. The same compositions were obtained either by melting of batches of initial compounds synthesized in advance or by solid state interaction at T = 330–350°C.

Thermograms of samples were taken on a Paulik–Paulik derivatograph (heating rate, 10°C min^{-1}). X-ray studies were carried out on a UPS-50 IM diffractometer with Cu$K\alpha$ radiation and a Ni filter. The IR spectra of glasses are taken on a UR-10 spectrophotometer (Karl Zeiss Jena) in the 1200–400 cm^{-1} range (1200–700 cm^{-1} NaCl prism, 700–400 cm^{-1} KBr prism). The samples were photometered in Nujol and for comparison in a KBr pellet. The wavenumber accuracy of recording of the absorption maxima was ±1.5 cm^{-1} for the crystalline samples and ±3 cm^{-1} for the glasses.

0022-4596/87 $3.00

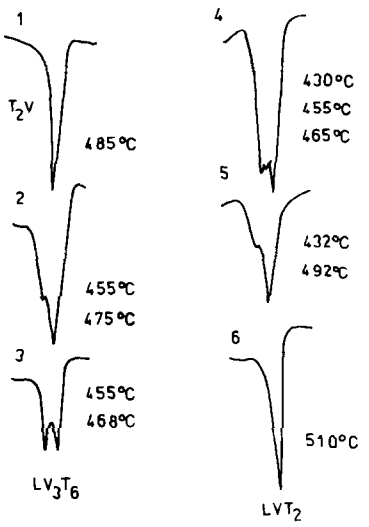

FIG. 1. Differential thermal analysis of compositions of the T_2V–LVT_2 system: 1—T_2V, 2—$2OLVT_2 \cdot 8OT_2V$, 3—LV_3T_6, 4—$4OLVT_2 \cdot 6OT_2V$, 5—$8OLVT_2 \cdot 2OT_2V$, 6—LVT_2.

Results and Discussion

(*a*) *Differential Thermal Analysis*

The thermograms of composition obtained for crystallized melts to the right of the presumed eutectic point, in the direction toward LVT_2, are characterized by two endothermic melting peaks (Fig. 1, No. 5). The first stays constant (435°C) but the second varies with the composition and corresponds to the liquidus temperature. The eutectic point lies at 40 mole% T_2V. The thermograms of compositions between the eutectic point and the composition of 66.6 mole% T_2V show two or three endothermic melting peaks (Fig. 1, No. 4). The first two do not change with the composition and correspond to the eutectic point (430°C) and the temperature of decomposition of incongruently melting phase LV_3T_6 (455°C), respectively. The third endothermic effect varies with the composition and for this reason it was related to the liquidus temperature. The thermograms of the composition of 66.6 mole% T_2V, corresponding to the new phase contains only two endothermic peaks, as expected, corresponding to the peritectic temperature and the liquidus temperature (Fig. 1, No. 3). The endothermic effects beyond the compound LV_3T_6 in the direction toward T_2V are two in number and correspond to the peritectic and liquidus temperature (Fig. 1, No. 2). The DTA results for compositions obtained by solid state reaction are similar. The phase diagram of the T_2V–LVT_2 system, built up on the basis of DTA data, is shown in Fig. 2.

(*b*) *X-Ray Diffraction Study*

The data from the X-ray diffraction study confirm the results obtained by DTA. The characteristic interplanar spacings of T_2V phase predominate at low concentrations. Gradually, along with them new reflection interplanar spacings also begin to appear. Their intensity increases while at composition LV_3T_6 they are the only ones remaining. Beyond this composition the interplanar reflections for the T_2V phase disappear, but those for the LVT_2 phase appear. The characteristic interplanar spacings of the new LV_3T_6 phase are compared to those of both the initial T_2V and LVT_2 phases in Table I.

(*c*) *IR Spectra of Crystalline Products*

The IR spectra of glasses and crystalline products of the T_2V–LVT_2 system are pre-

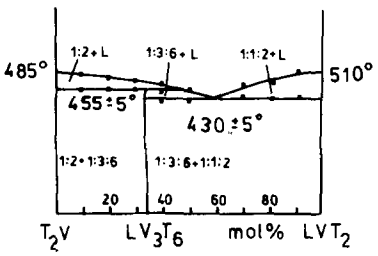

FIG. 2. Phase diagram of the $2TeO_2 \cdot V_2O_5$–$Li_2O \cdot V_2O_5 \cdot 2TeO_2$ system (T_2V–LVT_2).

TABLE I

INTERPLANAR SPACINGS (d_{obs}, Å) AND RELATIVE INTENSITIES (I/I_0) FOR T_2V, LVT_2, AND LV_3T_6

T_2V		LVT_2		LV_3T_6	
4.85	32	6.29	35	6.97	98
3.70	83	4.75	25	4.10	7
3.50	100	4.62	70	3.87	5
3.29	42	4.04	50	3.62	100
3.10	63	3.82	45	3.35	7
3.05	75	3.53	60	2.98	18
2.43	28	3.25	100	2.40	8
2.18	28	3.09	50	2.32	82
1.97	26	2.96	30	2.07	6
1.75	27	2.43	35	1.37	17

sented in Figs. 3 and 4. The IR spectra of the crystalline T_2V and LVT_2 phases were investigated earlier (*5–8*). As seen from Fig. 4, they exhibit characteristic bands, which are useful for their individual interpretation. The range of 1000–850 cm^{-1} is very peculiar in this respect. The doublet at 960–950 cm^{-1} appears to be characteristic of one of the T_2V phase, while the bands at 935–920 cm^{-1} and 880 cm^{-1} are associated with LVT_2.

As may be noticed from Fig. 3, with increasing Li_2O concentration in the direction toward T_2V, along with the characteristic bands of the latter compound, new ones with increasing intensity gradually appear, i.e., absorption peaks at 1003, 980, 965, 518, and 432 cm^{-1}. For the composition of 66.6% T_2V 33.3% LVT_2, these bands, together with the bands at 860, 822, 785, 765, 685, and 630 cm^{-1} are the only detectable ones in the spectrum (Fig. 4). Thus, the results of the DTA and X-ray diffraction analysis are confirmed; a new compound has been prepared. With a further increase in Li_2O concentration, bands characteristic of LVT_2 appear alongside the band of the new compound (Figs. 3 and 4). The ob-

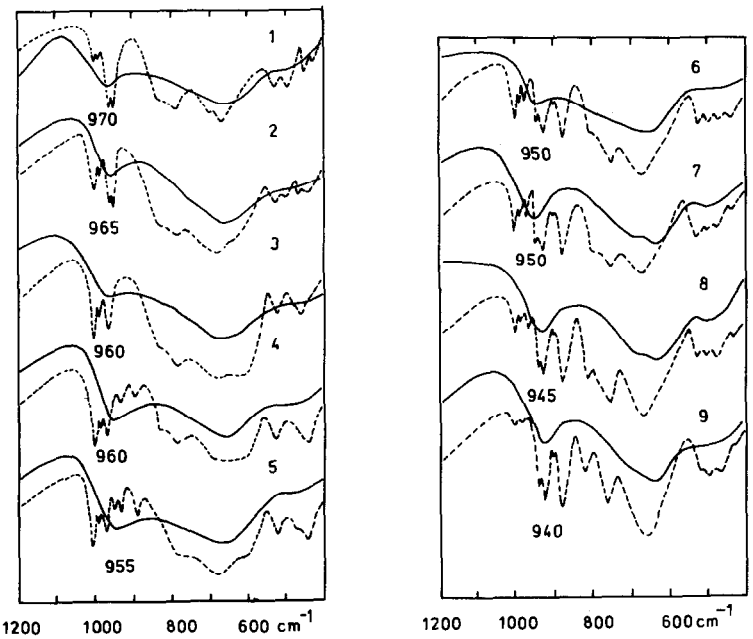

FIG. 3. Infrared spectra of compositions in the T_2V–LVT_2 system. 1—1OLVT$_2$ · 9OT$_2$V, 2—2OLVT$_2$ · 8OT$_2$V, 3—3OLVT$_2$ · 7OT$_2$V, 4—4OLVT$_2$ · 6OT$_2$V, 5—5OLVT$_2$ · 5OT$_2$V, 6—6OLVT$_2$ · 4OT$_2$V, 7—7OLVT$_2$ · 3OT$_2$V, 8—8OLVT$_2$ · 2OT$_2$V, 9—9OLVT$_2$ · 1OT$_2$V, glass (—), crystal (– – –).

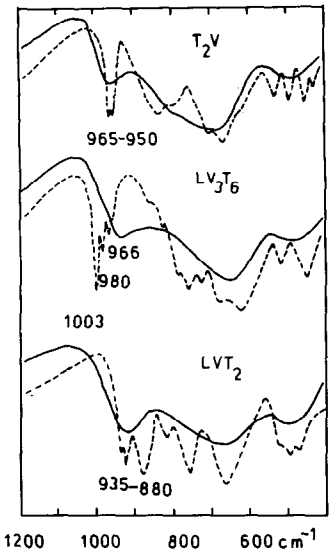

FIG. 4. IR spectra of stoichiometric compounds in the T_2V–LVT_2 system: glass (—), crystal (---).

served absorption bands for the three phases in this system are shown for comparison in Table II. In order to discuss the structure of the new compound a further examination of the structural and spectral data will be carried out.

The crystalline structure of the initial compounds T_2V and LVT_2 was investigated by Darriet (*9*, *10*). The chain structure of corner-shared VO_5 groups, each of which contains one nonbridging bond (1.63 Å), is characteristic of T_2V.

The individual V–O–V chains linked through Te_2O_5 groups are built up by two corner-shared TeO_3 groups, forming Te–O–Te bridges. The coordination polyhedra of V and Te with oxygen are preserved in the structure of the ternary LVT_2 compound (*10*), but in contrast to the T_2V structure they are not associated. Furthermore, two short nonbridging bonds (1.66 and 1.72 Å) in the VO_5 polyhedra exist. The peculiarities of both parent structures affect their IR spectra. As established in previous investigations (*5–8*) (Fig. 4), the intensive doublet band at 960–950 cm^{-1} in the T_2V spectrum is determined by the vibrations of nonbridging V–O bonds of the VO_5 groups. On the other hand, the symmetric and asymmetric stretching vibrations of both nonbridging V–O bonds from VO_5 groups in the LVT_2 structure exhibit absorption peaks at 935–920 cm^{-1} and 880 cm^{-1}.

The TeO_n polyhedra can be well characterized by the IR spectra (*7*, *8*). The Te_2O_5 groups in the T_2V show bands at 790, 720, 670, and 625 cm^{-1} assigned to $\nu^{s}_{TeO_2}$, $\nu^{as}_{TeO_2}$, ν^{as}_{TeOTe}, ν^{s}_{TeOTe} vibrations, while the TeO_3 groups in the LVT_2 are characterized by the bands at 750 cm^{-1} and 655 cm^{-1} assigned to ν^{s} and ν^{d} of the TeO_3 pyramid.

In the IR spectrum of the new LV_3T_6 phase three high-frequency bands are observed, at 1003, 980, and 966 cm^{-1}, in contrast to the $NV_3T_6(2)$ and $KV_3T_6(4)$ spectra, for which only two bands are observed.

The alkaline trivanadates exhibit similar spectra, as is shown in Ref. (*2*). In the spectra of the Rb and Cs trivanadates two bands in the 1000–900 cm^{-1} range exist, while in the LiV_3O_8 spectrum three high-frequency absorption maxima at 1000 cm^{-1}, 975 cm^{-1}, and 957 cm^{-1} appear (*11*). As to the structure, the alkaline trivanadates are built up

TABLE II

INFRARED ABSORPTION BANDS OF T_2V, LVT_2, AND LV_3T_6 CRYSTALS

T_2V (cm^{-1})	LVT_2 (cm^{-1})	LV_3T_6 (cm^{-1})
960–950	935–920	1003
830	880	980
790	810	966
720	750	860
670	665	822
625	480	785
525	460	765
495		732
450		685
425		630
		518
		432

from zigzag chains of V_2O_8 groups, each of which contains two equal nonbridging bonds. The individual chains are interconnected by VO_5 complexes, four oxygen atoms of which are common to adjacent V_2O_8 groups; the fifth oxygen forms an isolated V–O bond with a length of 1.58–1.63 Å. Whenever the dipoles are in opposite orientation at colinear nonbridging bonds in the V_2O_8 groups, these modes will be inactive in the IR spectrum, due to the interaction of the V–O stretching vibrations. This is the case with K, Rb, and Cs trivanadates. Here, aside from vibrations of the interacting V–O bonds from the V_2O_8 groups, an absorption maximum of the third V–O bond of the VO_5 group (*2*) in the 1015–1000 cm^{-1} range appears. The appearance of the third band in the LiV_3O_8 spectrum could be explained by the activation of ν^s in consequence of the lower symmetry of the V_2O_8 groups. The VO polyhedra, from which LV_3T_6 is built up, have a structure close to that of alkaline trivanadates. There are two types of vanadium–oxygen groups. On the one hand, there exist V_2O_8 groups with lower symmetry, for which both the ν^s and ν^{as} are active in the IR spectra at 980 and 966 cm^{-1}. Thus, the third band at 1003 cm^{-1} should be assigned to another vibration mode, that of a short nonbridging bond of an unassociated VO_5 group. On the other hand, one could imagine that Te_2O_5 groups are formed, as in T_2V. The existence of bands at 765, 685, 630, and 518 cm^{-1} is related to $\nu^s_{TeO_2}$, $\nu^{as}_{TeO_2}$, ν^{as}_{TeOTe}, ν^s_{TeOTe} (*7*). At the same time, it is interesting to note the strong increase in the intensity of the band assigned to ν^s_{TeOTe} and the shifting of ν^{as}_{TeOTe} and ν_{TeOTe} with respect to these in the T_2V spectrum. This fact could be explained by a perturbation of the linearity of the Te–O–Te bridges of the Te_2O_5 group in the structure of the new compound. A similar spectrum for $MgTe_2O_5$ was shown in (*12*) by Baran, which was interpreted in terms of the vibrations of Te_2O_5 group with nonlinear Te–O–Te bridges between both TeO_3 groups.

The relation between the observed IR spectra of the three crystalline phases and the corresponding vanadium–oxygen and tellerium–oxygen polyhedra is shown in Figs. 5a and 5b.

(d) IR Spectra of Glasses

The discussion on the glass structure is based on the comparison of their spectra with those of the crystalline phases (Fig. 3). The range of vibration of the isolated V–O bonds is particularly sensitive to structural changes. In this range at 975 cm^{-1} the vitreous T_2V exhibits a band which may be considered as a stretching vibration of the isolated V–O bond of the VO_5 polyhedra (*5*). The VO_2 group of the LVT_2 is characterized by a broad absorption band at 920 cm^{-1} (*6*).

The IR spectra of the glasses of the investigated system show a weak band at 515 cm^{-1}, a wide complex band in the 700–600 cm^{-1} range, and a band changing its location with composition from 970 to 940 cm^{-1} (Fig. 3).

The comparison of the glass spectra with those of both endmembers of the crystalline phases shows that a gradual transformation from a structure characteristic of LVT takes place in the glassy state, as shown in Figs. 5a and 5b. This is confirmed by the gradual displacement of the band at 975 cm^{-1}, associated with VO_5 groups of the T_2V, to 920 cm^{-1}, at the expense of the increase of the role of the VO_5 groups which contain two isolated bonds in the LVT_2 structure. On the other hand, the rise of the contribution of the band at 665 cm^{-1} in the range of Te–O vibrations shows that the number of isolated TeO_3 groups in the LVT_2-rich glasses is raised. It should be noted that no structural motifs characteristic of LV_3T_6 are formed, as the spectrum of the glass corresponding to a stoichiometric composition LV_3T_6 differs from that of the

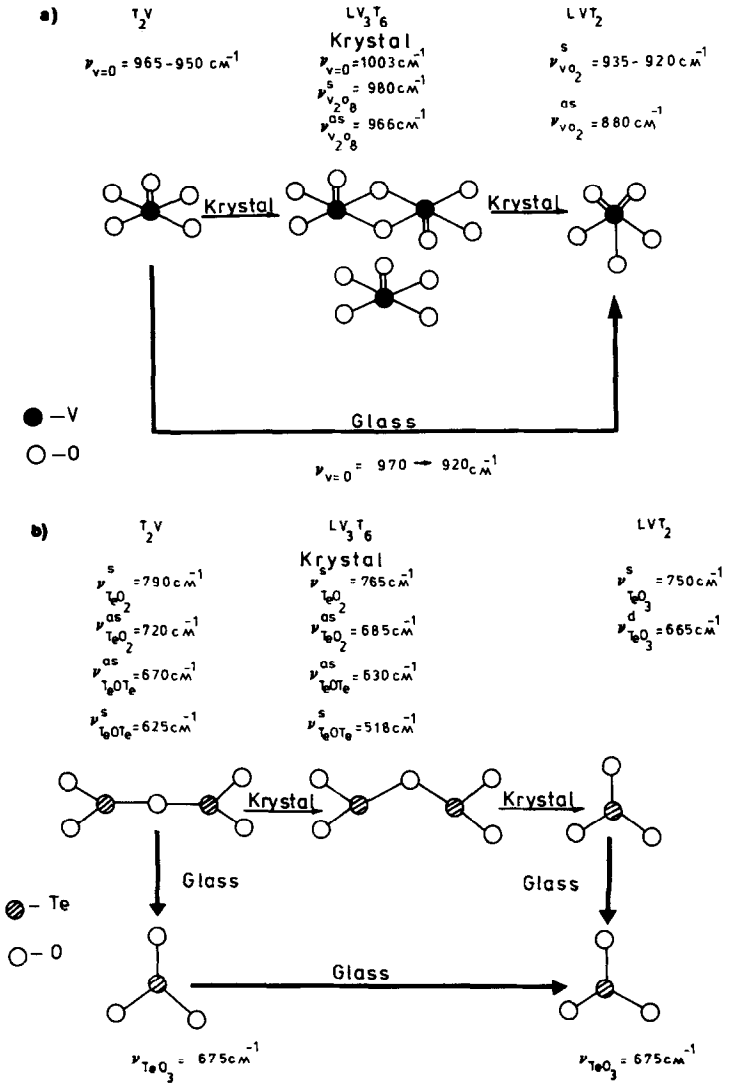

FIG. 5. Transformation scheme for structural polyhedra in the T_2V–LVT_2 system. (a) transformation of the VO polyhedra. (b) transformation of the TeO polyhedra.

crystalline phase. No bands above 960 cm^{-1} were found. This implies that, with respect to short-range order, the LV_3T_6 glass is closer to T_2V than to crystalline LV_3T_6, which is in accord with the phase diagram.

Conclusion

The phase diagram of the T_2V–LVT_2 was constructed. The formation of a new incongruently melting ternary compound of composition LV_3T_6 was established. Using IR spectroscopy, the basic structural units of the new phase, namely, VO_5, V_2O_8, and Te_2O_5 groups, were established.

With an increase of the Li_2O content, the structure of the glasses changes gradually. The VO_5 groups with one isolated V–O

bond (band at 975 cm^{-1}) transform to VO_5 groups with two isolated V–O bonds (band at 920 cm^{-1}).

References

1. J. Darriet, G. Guilloume, K. Wilhelmi, and J. Galy, *Acta Chem. Scand.* **26,** 59 (1972).
2. Y. Dimitriev, M. Arnaudov, and V. Dimitrov, *J. Solid State Chem.* **38,** 55 (1981).
3. Y. Ivanova and Y. Dimitriev, *Mater. Chem.* **6,** 287 (1981).
4. Y. Ivanova and V. Dimitrov, *J. Mater. Sci. Lett.* **2,** 541 (1983).
5. Y. Dimitriev, M. Arnaudov, and V. Dimitrov, *Mh. Chem.* **107,** 1335 (1976).
6. Y. Dimitriev, M. Dimitrov, and M. Arnaudov, *J. Mater. Sci.* **14,** 723 (1979).
7. M. Arnaudov, V. Dimitrov, Y. Dimitriev, and L. Markova, *Mater. Res. Bull.* **17,** 1121 (1982).
8. Y. Dimitriev, V. Dimitrov, and M. Arnaudov, *J. Mater. Sci.* **18,** 1353 (1983).
9. J. Darriet and J. Galy, *Cryst. Struct. Comm.* **2,** 237 (1973).
10. J. Darriet, *Bull. Soc. Fr. Mineral. Crystallogr.* **96,** 97 (1973).
11. Y. Kera, *J. Solid State Chem.* **51,** 205 (1984).
12. E. J. Baran, *Z. Anorg. Allg. Chem.* **442,** 112 (1978).